JOURNAL OF SOLID STATE CHEMISTRY 107, 381–386 (1993)

X-Ray Diffraction Analysis of the In/Ga and In/Al Interface Diffusion in Superlattices $(GaAs)_n(InAs)(AlAs)_n/GaAs(001)$ and $(AlAs)_n(InAs)(GaAs)_n/GaAs(001)$

JOSE FAYOS*

Instituto Rocasolano, Departamento de Cristalografía, CSIC, Serrano 119, 28006 Madrid, Spain

AND MERCEDES PEREZ-MENDEZ

Centro Nacional de Microelectrónica, CSIC, Serrano 144, 28006 Madrid, Spain

Received August 17, 1992; in revised form March 8, 1993; accepted March 11, 1993

Differences between In diffusion through InAs/AlAs and InAs/GaAs interfaces have been studied by X-ray diffraction in two crystals grown on GaAs(001) substrates by atomic layer molecular beam epitaxy. The two samples were designed to include one InAs layer into an AlAs/GaAs superlattice, the first in the growth sequence $(GaAs)_n(InAs)(AlAs)_n$ . . . and the second in $(AlAs)_n(InAs)(GaAs)_n$ . . . . It is shown that both growths produce the same extension In/Ga diffusion along five layers, although with different deformation of the interlayer spacings. © 1993 Academic Press, Inc.

Introduction

Previous characterizations of epitaxially grown superlattices by X-ray diffraction (XRD) (*1, 2*) have shown this technique to be useful to fit a growth model, even including some interface diffusion (*3*), which, nevertheless, is difficult to distinguish from interface roughness by this technique. The diffusion control of group III elements in III–V heterostructures is important for device performance. The aim of this work is to model by XRD the In/Al and In/Ga interdiffusion in two AlAs/GaAs superlattices with an InAs monolayer inserted before the AlAs barrier in the first and after it in the second. Both samples being grown by atomic layer molecular beam epitaxy (ALMBE) on GaAs(001) substrates (*4*).

* To whom correspondence should be addressed.

Experimental Superlattice X-Ray Spectra

Two samples, A and B, were grown by ALMBE with 36 periods in the sequences A: $(GaAs)_7(InAs)_1(AlAs)_8$ and B: $(AlAs)_8(InAs)_1(GaAs)_7$, both on GaAs(001) substrates at 400°C with a growth rate of 1 monolayer/sec. Plate-shaped fragments of these samples of $\sim$1 mm^2 were fixed to capillaries on their substrate side and mounted on a goniometer head with the superlattice (SL) growth direction ⟨001⟩ parallel to its rotation axis. The X-ray spectra were measured on a four-circle diffractometer so that the X-ray beam was always incident on the SL side. Cu$K\alpha$ graphite monochromated radiation was used at 25 mA and 50 kV. Once the SL unit cell had been oriented, the whole intensity profile from 2° to 68° (θ) along the ⟨001⟩SL direction was recorded in the $\theta/2\theta$ mode, using a 0.03° (2θ) step scanning, with 15 sec per step and a 0.5° (2θ) thin slit before the detector. The GaAs substrate peaks (S),

0022-4596/93 $5.00
Copyright © 1993 by Academic Press, Inc.
All rights of reproduction in any form reserved.

(002), (004), and (006), were also recorded with intensities ~20 times stronger than the corresponding SL zero orders, whose peaks could be separated in the recorded profiles from the (004)S and (006)S, but not from (002)S peaks.

The integrated XRD step-scanned intensities of the observed peaks in samples A and B were reduced to observed structure factors $F_{obs}(00l)$ by Lorentz and polarization corrections. No absorption correction was applied, as the usual procedures for plate-shaped samples did not work for this extremely thin one of ~1640 Å thickness. There were ~30 observed SL reflections, but those SL orders greater than 4 were not considered for the XRD analysis, as experimental growth defects reduce the intensity of high-order satellites (*2*). The reflections (003)SL were also rejected due to their proximity to the direct beam.

Results and Discussion

(*a*) *Analysis of the XRD Spectra*

The total number of layers in the unit cell for samples A and B was found to be 16 by indexing the satellites near (002)S as (0, 0, $16 \pm i$)SL (*1*). The superperiods C were measured using a finer scan around the (006)S peaks (0.01° (2θ) step scanning at 10 sec per step). The observed spacings of the (0, 0, 47), (0, 0, 48), and (0, 0, 49)SL peaks were corrected with the shifts observed for the (006)S of GaAs, and the C values were calculated as $48 \times [(d(0, 0, 47) + d(0, 0, 49))/2 + d(0, 0, 48)]/2$, being 45.49(1) Å for sample A and 45.53(2) Å for sample B. These C values predict distances between the satellites at both sides of the zero orders shorter than those observed, representative differences being for (0, 0, 16 ± 1)SL satellites of 0.04° in sample A and 0.10° in sample B. This incommensurability means that while the average heterostructure, obtained from the SL zero-order peaks, with a sublattice of ~5.6 Å, is quite periodic, it does not happen the same in the whole superlattice of ~45.5 Å, where some structural features, such as interface diffusion or interface roughness (*2*), are not so periodic along the growing direction.

It was also observed that the SL peaks were only 30% wider than the substrate ones, very narrow peaks indeed as compared with those of $(InAs)_8(AlAs)_2$ (*3*), which were 120% wider. Hence, the large size expected for the crystal domains in a GaAs/AlAs SL, due to the low lattice mismatch (a_0(GaAs) = 5.652 and a_0(AlAs) = 5.660 Å), does not decrease, as would be expected, when a monolayer of InAs (a_0(InAs) = 6.052 Å) is inserted. All of this suggests that some In diffuses within the lattices.

(*b*) *Fitting of the SL Growth Models to the Observed XRD Intensities*

Samples A and B were differently grown, and their observed XRD spectra are clearly different, as shown in Table I. We expected then to find two different growth models for them. Such models, including the above-mentioned In diffusion, would have three blocks: two with pure GaAs and AlAs and a third (mix) with atomic diffusion or statistically disordered (Ga/Al/In)As layers. The presence of both interfaces and diffusion, strain the crystals and deform the interlayer spacings $d_\perp$ of GaAs, AlAs, and InAs, which, together with the extent of the In diffusion, produce many variables to be fitted with the ~25 intensity data. Hence, we did two consecutive approaches to fit those models to the observed (00l) spectra.

In the first approach, the same partial populations for every chemical species p(Ga), p(Al), and p(In) are forced to be equal in every layer of the mix block. That is, a layer formula, $[GaAs]_{n(Ga)}[Ga_{p(Ga)}Al_{p(Al)}In_{p(In)}As]_{n(mix)}[AlAs]_{n(Al)}$, which corresponds to the growth direction of sample A from left to right, and from right to left for B. Hence the whole formula is $Ga_xAl_yIn_zAs_{16}$ where $x = n(Ga) + n(mix) \times p(Ga)$, $y = n(Al) + n(mix) \times p(Al)$, and $z = n(mix) \times p(In)$. We assumed $p(Ga) + p(Al) + p(In) = 1$ per layer, i.e., the total content of III-elements

TABLE I

LIST OF F_{obs} AND F_{cal} STRUCTURE FACTORS OF THE MODELS FOR SAMPLES A AND B, AFTER THE SECOND FITTING

	Sample A		Sample B	
l	F_{obs}	F_{cal}	F_{obs}	F_{cal}
3[a]	15	30	11	29
4	3	3	2	4
5[a]	4	19	5	18
8[a]	2	5		
11[a]	6	18	4	17
12	2	5	4	3
13	22	26	19	25
14	3	4	7	5
15	96	91	82	82
Z 16[a]		123		123
17	78	74	85	85
18	7	7	11	2
19	16	19	18	21
20	3	2	4	4
21[a]	5	12	6	13
22[a]	2	5		
25[a]			3	7
26[a]			3	4
27[a]	5	8	7	11
28	3	5	8	2
29	12	7	19	14
30	14	10	23	12
31	33	30	60	72
Z 32	357	359	373	370
33	76	77	24	28
34	18	10	12	6
35	9	19	7	13
36	5	5		
43[a]	3	5		
44	2	3		
45	7	8		
46	2	4		
47	29	26	14	19
Z 48	41	32	35	35
49	16	14	18	22
50	3	3	8	1
51	4	3		

Note. Z denotes the zero-order SL reflections.

[a] Reflections not used to refine the growth models, including the $l = 16$ which could not be separated from the (002) reflection of the substrate.

designed by ALMBE. The whole number of bilayers is $n(\mathrm{Ga}) + n(\mathrm{mix}) + n(\mathrm{Al}) = 16$, as experimentally proved in the above section. Finally, one bilayer spacing is considered for each species, $d_\perp(\mathrm{Ga})$, $d_\perp(\mathrm{Al})$, and $d_\perp(\mathrm{In})$, which should satisfy $x \times d_\perp(\mathrm{Ga}) + y \times d_\perp(\mathrm{Al}) + z \times d_\perp(\mathrm{In}) = C_{obs}$, or $n(\mathrm{Ga}) \times d_\perp(\mathrm{Ga}) + n(\mathrm{Al}) \times d_\perp(\mathrm{Al}) + n(\mathrm{mix}) \times d_\perp(\mathrm{mix}) = C_{obs}$ if we define the spacing of any layer in the mix block as $d_\perp(\mathrm{mix}) = p(\mathrm{Ga}) \times d_\perp(\mathrm{Ga}) + p(\mathrm{Al}) \times d_\perp(\mathrm{Al}) + p(\mathrm{In}) \times d_\perp(\mathrm{In})$.

In the second approach the mix block is relaxed. A variable $p_i(\mathrm{In})$ distribution is assumed along the best mix block of the previous fitting, plus one layer before and one after.

Initial values of $d_\perp(\mathrm{Ga})$ and $d_\perp(\mathrm{Al})$ were calculated as follows: $2d_\perp = a_0(1 + \mathscr{E}_\perp)$, where $\mathscr{E}_\perp = -\mathscr{E}_\parallel(2c_{12}/c_{11})$ and $\mathscr{E}_\parallel = (a_\parallel - a_0)/a_0$. a_0 is the unstrained periods already given above. $\mathscr{E}_\perp$ and $\mathscr{E}_\parallel$ are the normal strains and c_{12} and c_{11} are the elastic constants; $2c_{12}/c_{11}$ for GaAs and AlAs was calculated to be 0.901 and 0.865, respectively (*5–7*). Two values were considered for the deformed period parallel to the sample surface $a_\parallel$, first $a_\parallel = (7a_0(\mathrm{GaAs}) + 8a_0(\mathrm{AlAs}) + a_0(\mathrm{InAs}))/16$, as it was found for $(\mathrm{InAs})_8(\mathrm{AlAs})_2/\mathrm{GaAs}(001)$ (*3*); and second, the period of the substrate $a_\parallel^* = a_0(\mathrm{GaAs})$. The initial $d_\perp$ value for the minor and probably more strained component, InAs, was calculated to get C_{obs} for the SL period. In this way, the initial interlayer spacings sets for GaAs, AlAs, and InAs were [2.814, 2.822, 3.216 (for sample A) or 3.256 (for sample B) Å] and [2.826, 2.834, 3.036(A) or 3.076(B) Å], respectively, for $a_\parallel$ and $a_\parallel^*$.

The structure factors $F_{cal}(00l)$, for the first fitting approach, were calculated using the three terms corresponding to the GaAs, AlAs and mixed blocks:

$$F_{cal}(00l) = T[(f_{As} + f_{Ga}R_{Ga}^{1/2})(R_{Ga}^{n(\mathrm{Ga})} - 1)/(R_{Ga} - 1) + (f_{As} + f_{mix}R_{mix}^{1/2})R_{Ga}^{n(\mathrm{Ga})}(R_{mix}^{n(\mathrm{mix})} - 1)/(R_{mix} - 1) + (f_{As} + f_{Al}R_{Al}^{1/2})R_{Ga}^{n(\mathrm{Ga})}R_{mix}^{n(\mathrm{mix})}(R_{Al}^{n(\mathrm{Al})} - 1)/(R_{Al} - 1)].$$

Besides their atomic contents, the blocks are characterized by vectors $(R_i^{n(i)} - 1)/(R_i - 1)$, where i is Ga, Al, or mix, with

TABLE II

SOME GROWTH MODELS FOR SAMPLES A AND B IN THE FIRST APPROACH FITTING

	Sample	(%)	n(Ga)	n(Al)	n(mix)	p(Ga)	p(Al)	p(In)	x	y	z	$d_\perp$(Ga)	$d_\perp$(Al)	$d_\perp$(In)	B_T	R_F
(a)	A($a_\parallel$)		7	8	1	0	0	1	7	8	1	2.814	2.822	3.216	5.3	0.49
	($a_\parallel^*$)		7	8	1	0	0	1	7	8	1	2.826	2.834	3.036	1.6	0.35
(b)	B($a_\parallel$)		7	8	1	0	0	1	7	8	1	2.814	2.822	3.256	5.0	0.51
	($a_\parallel^*$)		7	8	1	0	0	1	7	8	1	2.826	2.834	3.076	2.5	0.33
(c)	A		7	8	1	0	0	1	7	8	1	2.826	2.856	2.860	1.7	0.24
	B		7	8	1	0	0	1	7	8	1	2.840	2.840	2.930	2.7	0.24
(d)	A		7	8	1	0.1	0.6	0.3	7.1	8.6	0.3	2.820	2.848	3.250	2.0	0.13
	B		7	8	1	0.6	0.1	0.3	7.6	8.1	0.3	2.840	2.840	3.140	4.2	0.13
(e)	A	17	6	8	2	0.2	0.4	0.4	6.4	8.8	0.8	2.820	2.848	3.250	3.0	0.11
		13	5	8	3	0.4	0.4	0.2	6.2	9.2	0.6	2.812	2.852	3.028	3.0	0.11
		21	4	8	4	0.4	0.2	0.4	5.6	8.8	1.6	2.812	2.856	2.882	3.0	0.10
	→	34	3	8	5	0.8	0	0.2	7	8	1	2.808	2.856	2.986	3.3	0.09
		15	2	8	6	0.8	0	0.2	6.8	8	1.2	2.800	2.856	3.002	3.0	0.10
	B	11	5	8	3	0.4	0.2	0.4	6.2	8.6	1.2	2.840	2.840	2.914	3.5	0.12
		19	4	8	4	0.4	0.2	0.4	5.6	8.8	1.6	2.840	2.840	2.896	3.5	0.12
	→	49	3	8	5	0.8	0	0.2	7	8	1	2.836	2.838	2.974	3.6	0.11
		21	2	8	6	0.8	0	0.2	6.8	8	1.2	2.824	2.840	3.006	3.6	0.13
(f)	A		3	8	5	0.8	0	0.2	7	8	1	2.822	2.848	2.966	3.5	0.14
	B		3	8	5	0.8	0	0.2	7	8	1	2.822	2.848	2.966	3.5	0.14

Note. → denotes the best solutions, which are the starting point for a second fitting of the distribution of p(In) in the mix block. The superlattice is divided into three blocks, for GaAs, AlAs, and diffused (mix) Ga/Al/InAs. $n(i)$ gives the number of layers which construct each block. $p(i)$ are the populations of the atoms Ga, Al, and In, in the (mix) block. The formula is $Ga_xAl_yIn_zAs_{16}$ and $d_\perp(i)$ are the interlayer spacings. B_T is the optimized temperature factor and R_F is the agreement factor between F_{obs} and F_{cal}. On the lines (e), the (%) represent the percentage of solutions (among the best 50) with the following $n(i)$ values.

differences of phase of $R_{Ga}^{n(Ga)}$ and $R_{Ga}^{n(Ga)}R_{mix}^{n(mix)}$ in between, where $R_i = \exp(2\pi i l d_\perp(i)/C)$. The atomic scattering factors are f_{As}, f_{GA}, f_{Al}, and $f_{mix} = p(Al)f_{Al} + p(Ga)f_{Ga} + p(In)f_{In}$. T is the temperature factor given by $T = \exp(-B_T \sin^2 \theta(00l)/\lambda^2)$, where B_T was optimized for any considered solution.

Taking into account the first approach conditions, besides B_T, there are six independent variables in $F_{cal}(00l)$, which could be n(Ga), n(Al), p(Ga), p(Al), $d_\perp$(Ga), and $d_\perp$(Al), the first four reducible to two if the total epilayer formula is fixed. Table II shows the results of the first fitting approach, whose steps are described below. The first structure factors calculations were done assuming the formula $Ga_7Al_8InAs_{16}$, no In diffusion, and the two initial spacing sets for $a_\parallel$ and $a_\parallel^*$, lines (a) and (b). Besides their high discrepancy R-factors ($R_F = \Sigma|F_{obs} - |F_{cal}||/\Sigma F_{obs}$), they point to $a_\parallel^*$ as the better option, which consequently was taken for next calcuations. Second, the spacings $d_\perp$(Ga) and $d_\perp$(Al) were relaxed by calculating structure factors for all possible combinations of values in the range $2.80 < d_\perp(Ga) < d_\perp(Al) < 2.86$ Å at intervals of 0.004 Å. The combinations giving the lowest R-factors are those in Table II(c). Next, four variables were taken, the above spacings plus the populations p(Ga) and p(Al) in the mix block, which were varied in the range $0 < p(i) < 0.9$ at intervals of 0.1. Table II(d) shows the best solutions that correspond to a low content of In, as it is $p(In) \times n(mix)$. Then, structure factors were calculated for all possible combinations of values for the six independent variables, with the following ranges and intervals (in the last parentheses): $0 < n(i) < 15$ (1), $0 < p(i) < 0.9$ (0.2), and $2.80 < d_\perp(Ga) < d_\perp(Al) < 2.86$ Å (0.004 Å). There were 180,200 such combinations, all the possible growth models in this approach, the best 50 of which, with $R_F < 0.110$ for sample A and $R_F < 0.124$ for sample B, were analyzed. Table II(e) shows, under (%), the percentage of solutions having the following $n(i)$ values, among the 50 best solutions. In the rest of the columns of Table II(e) are the correspondent best solutions for the other variables. These n-

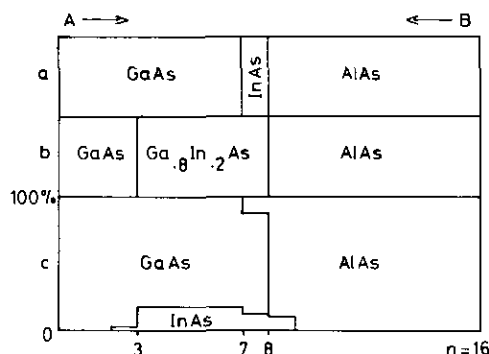

FIG. 1. Interface In diffusion for samples A and B. The arrows at the top indicate the respective growth directions: (a) the designed layer structure by ALMBE assuming no diffusion; (b) the first fitting approach of the diffusion to the XRD data, assuming the same formula for all layers in the mixed block; and (c) the second approach, fitting also the formula per layer. In each section, the vertical axis indicates the contents of each species GaAs, AlAs, and InAs per layer; the horizontal axis represents the total period of 45.5 Å or 16 bilayers.

set distributions show considerable In/Ga diffusion in both samples A and B, the best sets (with → in Table II) being n(Ga) = 3, n(Al) = 8, and n(mix) = 5. It is significant to show that, although there are some solutions with less In/Ga diffusion (specially for sample A), only the above (3, 8, 5) best n-set matches the expected chemical formula. Figure 1b shows this interface diffusion compared with the expected layer structure of Fig. Ia, where no diffusion is assumed.

As the best models for samples A and B only differ in their values of $d_\perp(i)$, we found of interest to calculate the F_{cal} of a common model by averaging these $d_\perp(i)$ between A and B. The Table II(f) shows the same fit between this model and both observed spectra, R_F being significantly worse than the above best solutions (→). This would confirm that the differences in the observed spectra are due to the two different deformations of the interlayer spacings in A and B, produced by its two inverted direction of growth. Although In interchanges with Ga in any case, the interlayer spacings of the superlattice become more homogeneous when, as in B, In diffuses in the direction of the growth.

The best solutions reached by the above first fitting, i.e., those (3, 8, 5) n-sets in Table II(e), were the starting points for the second fitting approach, where it was assumed a continuous In diffusion along seven layers, two more than the best n(mix), with the formula

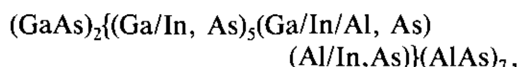

$$(GaAs)_2\{(Ga/In,\ As)_5(Ga/In/Al,\ As)(Al/In,As)\}(AlAs)_7,$$

which seems reasonable for a favored Ga/In interdiffusion. Then, the atomic populations of every layer in the diffused { } block were least squares refined (8). Both, the assumed formula, the best B_T values and the best $d_\perp$-sets of the first fitting approach, were fixed; and p_i(In) were constrained to increase from the borders of the diffused block to the (Ga/In/Al, As) layer. These refinements gave the same diffusion profile for the samples A and B,

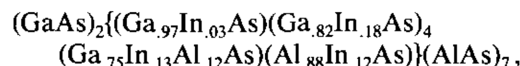

$$(GaAs)_2\{(Ga_{.97}In_{.03}As)(Ga_{.82}In_{.18}As)_4(Ga_{.75}In_{.13}Al_{.12}As)(Al_{.88}In_{.12}As)\}(AlAs)_7,$$

which shows no significant difference with the flat solutions imposed by the first fitting approach, having also the same R-factors, 0.09 and 0.11, respectively, for both samples. Table I lists the observed F_{obs} and the calculated F_{cal} after this second fitting of the models, which corresponds to the interface diffusion shown in Fig. 1c.

Conclusions

The observed periods C_{obs} of the superlattices GaAs/InAs/AlAs (A) and AlAs/InAs/GaAs (B) are very close, suggesting similar contents in the cell. The best structural models fitting the observed XRD spectra confirm the expected formula for both $Ga_7Al_8InAs_{16}$, with the same In/Ga diffusion along five layers, but obviously in the opposite direction. This fitting also shows that significant differences between the observed spectra of A and B are due to different deformation of their interlayer spacings, which become more simi-

lar if In diffuses, as in B, in the growth direction. About the ambiguity between diffusion and interface roughness, two facts support In diffusion. First, the narrow SL peaks observed, which would correspond to large crystal domains, due to the relaxation of the lattice mismatch by In diffusion. Second, the preference of the In/Ga interface diffusion versus the In/Al, which seems to be unrelated with any interface roughness during the sample growth. Finally, the high-temperature factors optimized to $B_T = 3.5$ Å^2 and the observed SL incommensurability are probably due to the atomic random disorder caused by the In/Ga diffusion.

Acknowledgment

The authors thank the Centro Nacional de Microelectronica in Madrid for providing the samples.

References

1. J. Kervarec, M. Baudet, J. Caulet, P. Auvray, J. Y. Emery, and A. Regreny, *J. Appl. Crystallogr.* **17,** 196 (1984).
2. P. Auvray, M. Baudet, J. Caulet, and A. Regreny, *Rev. Phys. Appl.* **24,** 711 (1989).
3. J. Fayos and M. Perez-Mendez, *Thin Solid Films* **189,** 329 (1990).
4. F. Briones, L. Gonzalez, and A. Ruiz, *Appl. Phys. A* **49,** 729 (1989).
5. C. W. Garland and K. C. Park, *J. Appl. Phys.* **33,** 759 (1962).
6. Landolt-Bornstein, "Semiconductors: Technology of III–V, II–VI, and Non-tetrahedrally Bonded Compounds," Vol. 17d, p. 14, Springer, Berlin (1984).
7. A. Segmuller, P. Krishna, and L. Esaky, *J. Appl. Crystallogr.* **10,** 1 (1977).
8. J. M. Stewart, F. A. Kundell, and J. C. Baldwin, "The XRAY-80 System," Computer Science Centre, Univ. of Maryland, College Park (1980).